GEOPHYSICS, VOL. 58, NO. 4 (APRIL); P. 534–543, 13 FIGS.

Wave propagation effects on amplitude variation with offset measurements: A modeling study

Ruben D. Martinez*

ABSTRACT

Wave propagation effects can significantly affect amplitude variation with offset (AVO) measurements. These effects include spreading losses, transmission losses, interbed multiples, surface multiple reflections, *P-SV* mode converted waves and inelastic attenuation.

Examination of prestack elastic synthetic seismograms suggests that spreading losses and the transmission losses plus compressional interbed multiples are manifest mainly as a time and offset effect on the primary reflections. The surface related multiples and the *P-SV* mode-converted waves interfere with prestack amplitudes inducing distortions in the AVO pattern. Such distortions cause large variances in AVO model fitting. Prestack viscoelastic synthetic seismograms also suggest that inelastic attenuation further complicates the AVO response because of the offset and time variant amplitude decay effects and the phase change due to dispersion. Together, all these effects severely alter AVO behavior and result in serious errors in AVO parameter estimates being made from inadequately corrected seismograms.

This modeling study suggests that time and offset dependent data processing prior to AVO analysis would be necessary to correct for the wave propagation effects, via either inverse filtering or model based approaches.

Comparisons between acoustic and elastic synthetic seismograms show that corrections for the wave propagation effects derived using acoustic approximations are inadequate. Corrections need to be calculated based on elastic approximations provided that the inelastic attenuation effects have been previously removed.

INTRODUCTION

Reflection coefficients vary as a function of offset (or ray parameter or incidence angle) due to elastic parameter changes across an interface. These changes may be used to infer fluid and/or lithologic changes from one geologic formation to another (Rutherford and Williams, 1989; Ostrander, 1984; Silva and Ahmed, 1989; Chacko, 1989). However, many other factors also affect the amplitude variation with offset (AVO) information. These may be classified into the following four categories: (1) data collection, (2) data processing, (3) geologic, and (4) wave propagation effects (Sheriff, 1975). Additionally, the traveltimes associated with these amplitudes also experience these effects in the form of time delays (Byun and Young, 1989). These kinematic effects are not discussed in this paper. The analyses presented here are only confined to the wave propagation effects on amplitudes.

Some of the important data collection factors that affect AVO measurements are: source directivity, source and receiver arrays, and source and receiver coupling. These effects have already been discussed in the literature, and most of them can be corrected deterministically and/or statistically by means of inverse operations (Gassaway et al., 1986; Krail and Shin, 1990; Ostrander, 1984).

In data processing, the AVO effects may be altered due to the erroneous selection of processing parameters and sequences. Amplitude misadjustments may be induced during the application of processes such as: scaling (e.g., trace equalization), deconvolution, normal moveout (NMO) stretching, filtering operations (e.g., *f-k* velocity filtering), etc.. Other sources of potential amplitude distortions include NMO velocity errors (Swan, 1991; Spratt, 1987), offset to incidence angle transformations, etc..

The data processing effects on AVO can be minimized by carefully selecting the processing parameters and sequences

Manuscript received by the Editor October 23, 1991; revised manuscript received September 3, 1992.
*Halliburton Geophysical Services, One Fluor Daniel Dr., P.O. Box 5019, Sugarland, TX 77487-5019.

(Yu, 1985) and by calibrating the processing results with prestack synthetic seismograms. The normal moveout (NMO) stretching problem and NMO velocity errors are major problems in this category. Swan (1991) provided a comprehensive analytical treatment of these problems and showed that the NMO velocity errors are the most serious in affecting the AVO analysis results.

The geologic effects on AVO signatures are unavoidable but need to be considered. These effects are mainly induced by geologic dip (Resnick et al., 1987), reflector curvature (MacLeod and Martin, 1988), tuning due to thin layering (Swan, 1991), and isochron distortions due to shallower anomalies (e.g., shallow gas pockets)(Gassaway, 1985). The structural complexity can be accounted for in the incidence angle calculations (Resnick et al., 1987). Prestack imaging (e.g., dip moveout) helps to reduce the effects of bed curvature (MacLeod and Martin, 1988). The tuning due to thin layering and interference effects are difficult to remove. The presence of these effects depends on the frequency content of the data.

The wave propagation effects may also be regarded as geologic effects, since it is the geologic setting which causes them. They may also be called overburden effects since they are caused by the overlying geologic conditions.

Some of the most important wave propagation effects are: spreading losses, transmission losses plus interbed multiples due to fine layering (also known as stratigraphic filtering) (Pruessmann and Behle, 1990), surface multiple reflections, P-SV mode-converted waves, and inelastic attenuation (Q effects). These effects are complicated functions of time and offset. The relative impact of these effects on AVO measurements is analyzed in this paper by making use of acoustic, elastic, and viscoelastic prestack synthetic seismograms. The results suggest that the removal of these effects is necessary to correctly derive the AVO attributes.

A comparison of acoustic with elastic responses is analyzed, and the results indicate that corrections for the wave propagation effects must be based on elastic approximations and not on acoustic approximations provided that the inelastic attenuation effects were removed.

PRESTACK MODELING

The prestack modeling performed in this study is based on the reflectivity method (Fuchs and Muller, 1971; Kennett, 1979). Several assumptions are made here for elastic and viscoelastic modeling: (1) the earth model layers are parameterized by P-wave velocity, S-wave velocity, density, P-wave quality factor, S-wave quality factor, and layer thickness; (2) the layers are isotropic and homogeneous; (3) the layers lie between upper and lower half-spaces; and (4) transmission effects, interbed multiples, free surface multiples and P-SV conversions are included in the synthetic seismogram calculations. Details of the algorithms are described in Martinez and McMechan (1987 and 1991a).

For this study, acoustic, elastic, and viscoelastic prestack synthetic seismograms were generated. The effects included in the synthetic seismograms were: spreading losses (since point source seismograms were calculated), transmission losses plus interbed multiples, surface multiples, P-SV wave mode conversions, and inelastic attenuation. No transverse isotropy was included in the calculations.

The earth model used to generate the prestack synthetic seismograms consisted of 471 isotropic and homogeneous layers characterized by: P-wave velocity, density, Poisson's ratio, P and S quality factors (Q_P and Q_S), and layer thicknesses (Figure 1). The P-wave velocity log was derived from a sonic log and subsequently block averaged to keep only those layers (thick and thin) that showed relatively large fluctuations in P-wave acoustic impedance (calculated using the P-wave velocity and density logs). Unfortunately, the density log was not recorded over the same depth interval as the sonic. A constant density value of 2.18 g/cm^3 was used for the upper zone where no density information existed. However, the depth range of the recorded density log constrained the studied region.

The Poisson's ratio log was computed using the empirical formulas given in Han et al. (1986). These formulas parameterize the P- and S-wave velocities (V_P and V_S, respectively) as linear functions of shale volume (V_{SH}) and porosity and are valid for shaly sand sequences. In this case the gamma ray and sonic logs were used to calculate V_{SH} and V_P, respectively. Having V_{SH} and V_P, the porosity was calculated directly with the first Han's empirical formula which relates V_{SH} and porosity with V_P. V_S was computed using both V_{SH} and porosity by means of Han's second empirical formula which relates V_{SH} and porosity with V_S. The Poisson's ratio was then calculated from V_P and V_S (Figure 1). The target zone is indicated by the arrow in Figure 1, which corresponds to a clastic reservoir.

The Q_P (P-wave quality factor) model was obtained from the P-wave velocities by dividing the interval velocities in ft/s by 100. The Q_S (S-wave quality factor) model was derived from the P- and S-wave velocity and the Q_P models using the following relationship,

$$Q_S = \frac{Q_P}{3/4(V_P/V_S)^2}.$$

This relationship assumes that the energy losses in pure compression are small (Dohr, 1985), i.e, the anelastic behavior of the shear modulus is the main factor responsible for the seismic wave attenuation. The synthetic seismograms were computed in the offset region of 1487 to 7434 ft (453 to 2265 m). However, the AVO analysis was performed in the offset region of 1487 to 5455 ft (453 to 1662 m), which correspond to approximately 7 and 25 degrees incidence angle, respectively, at the target zone (1720 ms, approximately). The use of this offset (angle) range in AVO analysis is to comply with the assumptions of Shuey's approximation (Shuey, 1985). The sampling rate was 4 ms, and the synthetic seismograms were filtered with a zero-phase band-pass filter of 8-75 Hz which simulates a source wavelet.

PRESTACK SYNTHETIC SEISMOGRAMS ANALYSIS RESULTS

Plane wave versus point source seismograms

The spreading losses are generally only partially corrected in data processing. The conventional time scaling applied to correct this effect is not sufficiently accurate when the seismic data is to be used for AVO analysis. The spreading

losses can be corrected by either using a rigorous approach (Ursin, 1990) or an approximation. In this case, the offset dependent approximation given by Ursin [1990, his equation (23)] is employed. This approximation should be sufficient for the range of incidence angles normally used in AVO analysis when an AVO model such as Shuey's (1985) is used. The rms velocities required by this process were derived from the model's interval velocities.

Figure 2 shows a comparison, through the zone of interest, of the elastic plane-wave response calculated using the Zoeppritz equations (c.f., Berkhout, 1987 p. 218) (Figure 2a), with the elastic point source response corrected for the offset dependent spreading losses only (Figure 2b). Both seismograms were only computed for primary events with no transmission losses, that is, no wave propagation effects were included. The target event (trough) is indicated by the arrow. The similarity between the two responses is quite good.

The absolute amplitudes of the target event were picked and plotted (Figure 3). Good agreement is observed between the curves showing the plane wave (a) and the corrected point source (b) amplitudes. The uncorrected point source amplitudes are shown on the same plot (Figure 3) for comparison. These amplitudes were normalized to the corrected point source amplitude of the first trace. The offset-dependent difference observed on the plot, emphasizes the importance of the offset-dependent spreading loss correction to preserve the correct AVO response.

Transmission losses plus compressional interbed multiple effects

The prestack synthetic seismogram shown in Figure 2b was further complicated with transmission losses and compressional interbed multiples (Figure 4). The effect of the fine layering overlying the target horizon is clearly observed. Figure 5 shows the amplitudes picked for the spreading loss-corrected point-source response, with the amplitudes containing transmission losses plus compressional interbed multiples.

Three main points from this comparison are: (1) all the amplitudes (crosses) are lower than the primary amplitudes (squares) as a result of the transmission losses; (2) there is a slight relative decrease of amplitude (crosses) with offset due to the offset dependency of the transmission losses; (3) the oscillations observed (crosses), are a result of interference from compressional interbed multiples generated at the layers above the target.

Compressional surface multiples and *P-SV* wave mode conversions

More wave propagation complexities were added to the seismogram shown in Figure 4. Figure 6a shows the seismogram with the inclusion of surface multiples. At this level of complexity, the surface related multiples are compressional only. The amplitudes picked at the target horizon (Figure 7)

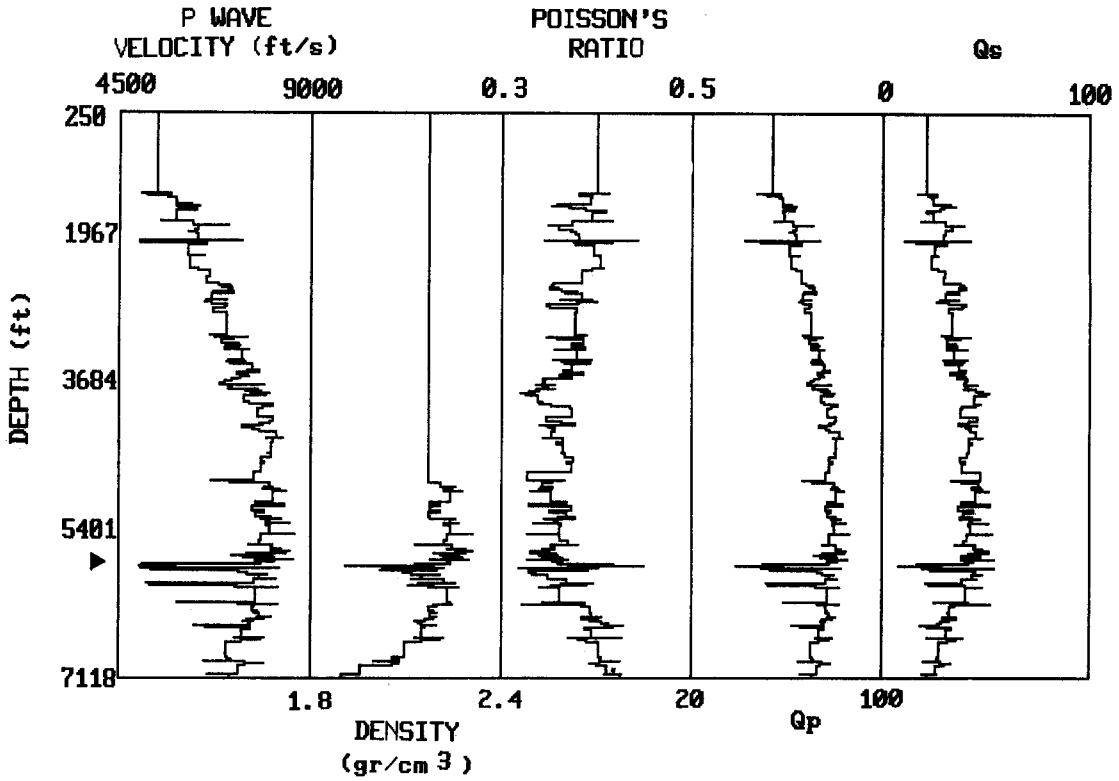

FIG. 1. Earth model used to compute the prestack synthetic seismograms. The model is characterized by 471 isotropic and homogeneous layers.

show considerable oscillations as a result of the interference from multiples originating in the shallower region of the earth model.

The impact of this effect on the AVO attribute estimations was that large variances were induced when fitting an AVO model to the amplitudes. In this case, the oscillations were larger than those observed for the case of transmission losses plus compressional interbed multiples, and would introduce errors in the estimated AVO parameters (Walden, 1990).

The additional inclusion of P-SV mode-converted waves induces even more complicated interferences on the primaries. At this level of complexity the interbed and surface multiples now experience the wave conversions from P to SV as well. The synthetic seismogram is shown in Figure 6b. Differences are observed with respect to the seismogram

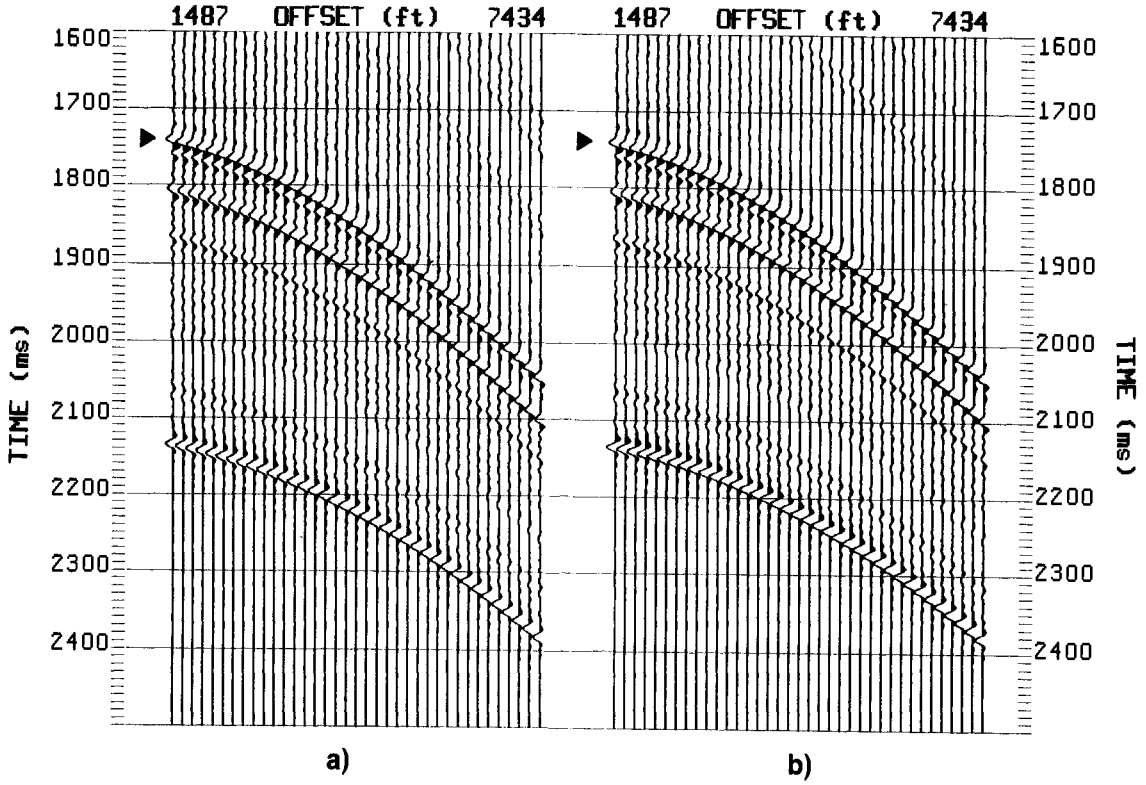

FIG. 2. Prestack elastic synthetic seismograms featuring the plane-wave response (a) and the point-source, response-corrected for spreading losses (b). The arrow indicates the target horizon.

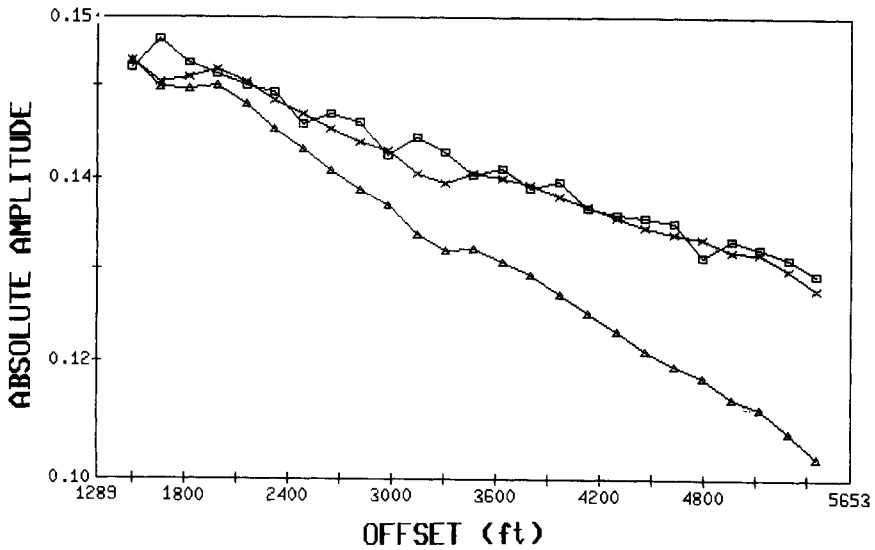

FIG. 3. Amplitude variations with offset picked at the target horizon using the seismograms shown in Figure 2a (squares) and 2b (crosses). The uncorrected point source amplitudes (triangles) are also shown for comparison.

shown in Figure 6a. However, the AVO trend shows an emphasized decrease of AVO caused by the *P-SV* mode conversions interferences (Figure 7).

From Figure 7 it is evident that the major wave propagation effects observed so far on the synthetic seismograms are the transmission losses plus compressional interbed multiples.

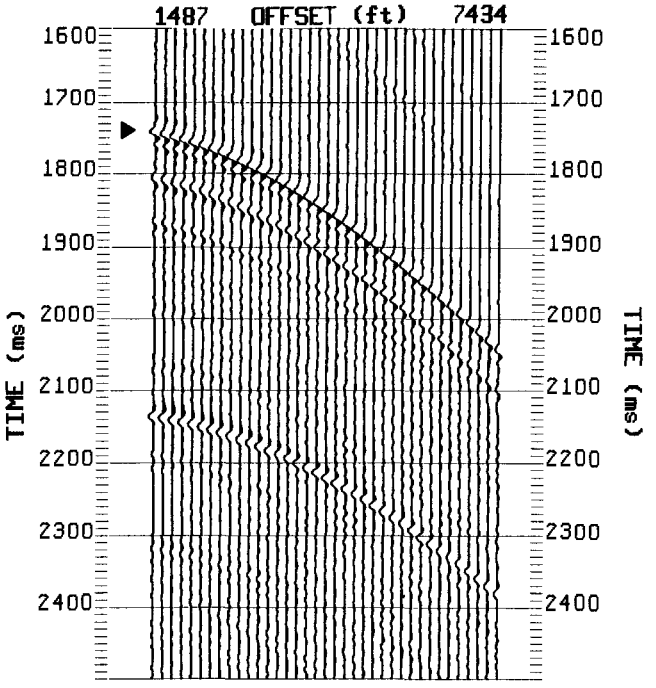

FIG. 4. Prestack elastic synthetic seismogram. The seismogram includes primaries plus transmission losses and compressional interbed multiples. The arrow indicates the target horizon.

Inelastic attenuation effects (*Q* effects)

The seismogram shown in Figure 6b was further complicated with Q effects, inducing significant amplitude decay high-frequency loss, and phase variations as observed in the synthetic response (Figure 8).

Figure 9 shows the plot of the amplitudes picked at the target horizon. The amplitudes were normalized based on the primary amplitude, with no effects, at zero offset. A large departure from the AVO trend shown by the primary amplitudes is observed due to the scaling applied during the normalization step. The Q effects attenuate the large oscillations caused by the surface related multiples and the *P-SV*-wave mode conversions, thereby reducing the variance of the AVO estimates, but still yielding erroneous AVO parameter estimates. More importantly, when Q effects are present, the reflection coefficients, in the precritical region, no longer have zero-phase conditions. Since the Q effects are linked to dispersion, phase variations are introduced. These amplitudes are not appropriate for AVO studies using elastic theory or any of its approximations.

AVO ANALYSIS RESULTS FOR THE TARGET HORIZON

To summarize the wave propagation effects on AVO measurements, a conventional AVO analysis was performed using Shuey's AVO approximation (Shuey, 1985). This approximation to the Zoeppritz equations is given by,

$$R(\theta) = R_0 + G_r \operatorname{Sin}^2 \theta,$$

where $R(\theta)$ are the reflection coefficients varying as a function of the incidence angle θ; R_0 is the P reflection coefficient or P-wave estimate at zero offset (or zero incidence angle); and G_r is the AVO gradient (slope).

Figures 10 and 11 show the P-wave and absolute AVO gradient least-squares estimates with their corresponding standard deviations in histogram form. Each pair of bars represent the wave propagation effects discussed above. The first pair, in both figures, corresponds to the primaries only,

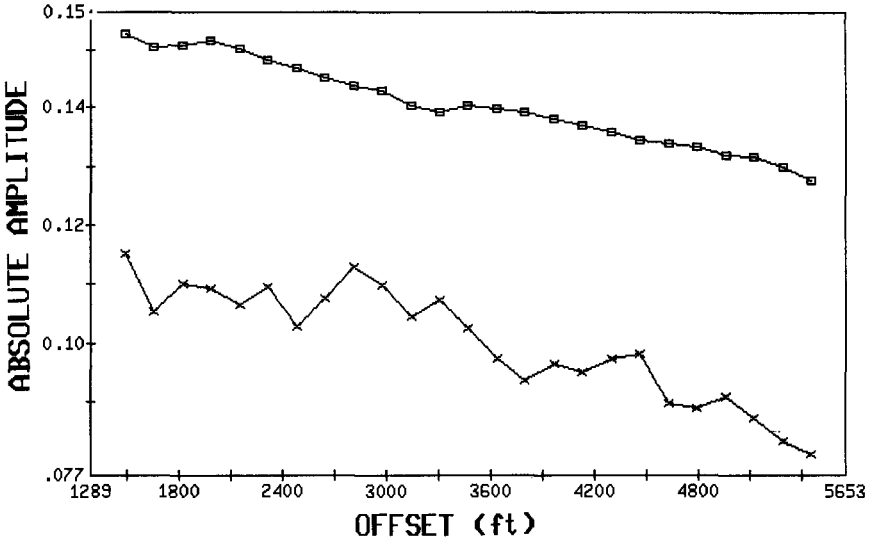

FIG. 5. Amplitudes versus offset picked at the target horizon using the seismograms shown in Figure 2b (squares) and Figure 4 (crosses).

and represents the ideal answer from the AVO analysis. The standard deviation for both parameters is relatively small, as would be expected.

Continuing to the right, in both Figures (10 and 11), the second pair of bars is the estimated parameters when transmission losses and compressional interbed multiples are included. As expected, the *P*-wave amplitude is reduced due to the transmission through the layering above the target zone (although some amplitude build up is present because of interbed multiple superposition). The absolute AVO gradient (Figure 11) experiences an increase with respect to the estimated gradient of the primaries with no effects. This demonstrates the offset dependent nature of the transmission losses. The standard deviation is larger than that of the primaries only due to the interference induced by the compressional interbed multiples generated above the target zone.

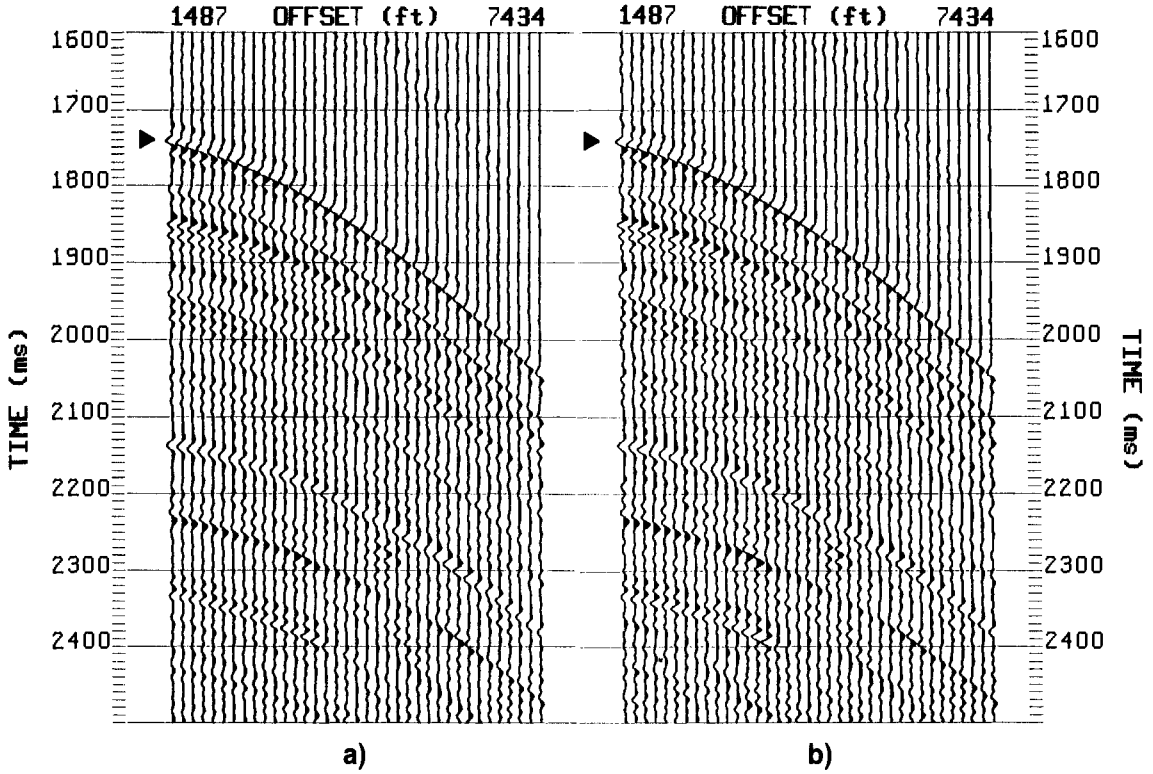

FIG. 6. Prestack elastic synthetic seismograms: (a) includes the same effects as the seismogram shown in Figure 4 plus compressional surface related multiples; (b) includes the same effects as in (a), but with the inclusion of *P-SV* mode converted-waves (including multiples). The arrow indicates the target horizon.

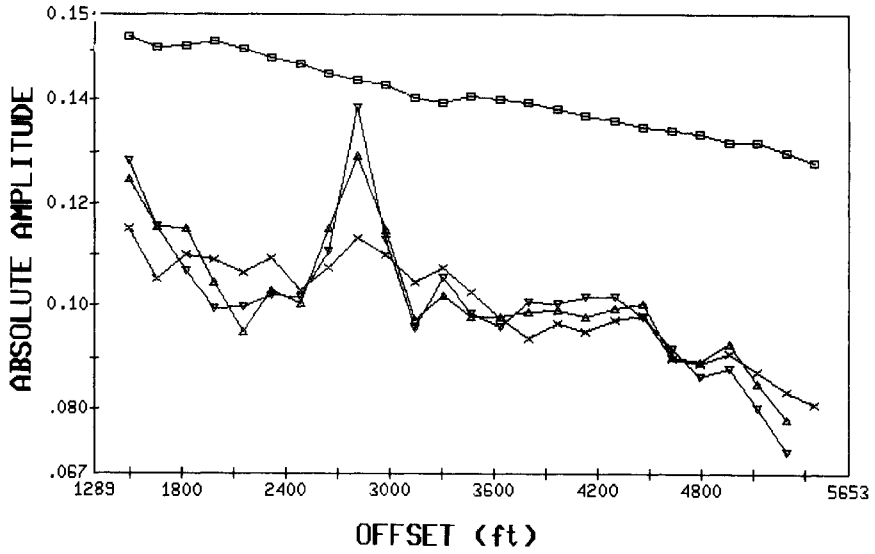

FIG. 7. Amplitudes variation with offset picked at the target horizon using the seismograms shown in Figures 6a (triangles) and 6b (upside down triangles). The amplitude plots from Figure 5 were repeated for comparison.

The inclusion of surface related multiples and *P-SV*-mode-converted waves does not have a significant effect on the *P*-wave estimates (third and fourth bar pairs in Figures 10 and 11).

The absolute AVO gradient estimate was affected more by the interferences created by the multiples and/or converted waves originated in the overburden, as previously described. This effect is reflected by the standard deviations, which are largest. For both the *P*-wave and the AVO gradient estimates, if the primary coincides in time with a multiple or a converted wave, then a complex situation arises, and the AVO analysis results will be in error.

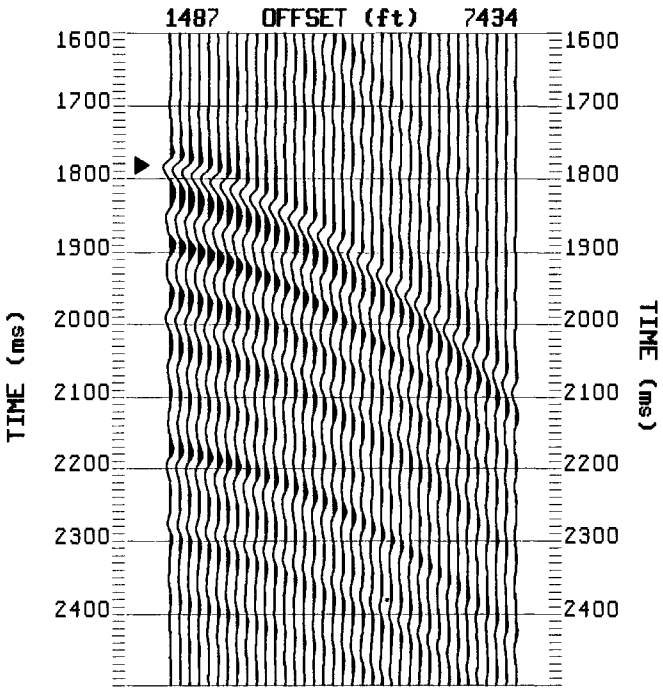

FIG. 8. Prestack viscoelastic synthetic seismogram that includes all the effects of the seismogram shown in Figure 6b plus inelastic attenuation effects. The arrow indicates the target horizon.

The Q effects (Q_P and Q_S) have the largest impact on both the *P*-wave and absolute AVO gradient estimates (Figures 10 and 11). The *P*-wave amplitude becomes heavily reduced, as expected. The AVO gradient also experiences a large change and it almost approaches zero. Note that the standard deviation is small for both the *P*-wave and the absolute AVO gradient. This points out a pitfall in the AVO parameter estimation, that is, the standard deviation cannot be uniquely used as an indicator of reliable parameter estimates, but just as a diagnostic of the goodness of fit.

Figures 9 and 11 may appear to be contradictory because in Figure 9 the AVO gradient seems large, while in Figure 10 the absolute AVO gradient is almost zero. The explanation for this is in the scaling applied to the *P*-wave amplitudes (with all wave propagation effects) in Figure 9. The scaler was computed to match the primary amplitude (with no wave propagation effects) when both amplitudes were extrapolated to zero offset.

Since this scaling was equally applied to the nonzero offset traces of the gather, a large change is caused in the original AVO gradient regardless of its original small magnitude. This resembles what is frequently observed on real seismic data whose amplitudes are scaled versions of the earth's response in reflectivity units.

This example points out that scaling of the data to recover the *P*-wave amplitude, without correcting for the offset dependency of the amplitude, frequency, and phase due to Q effects, is not appropriate and yields erroneous AVO gradient estimates.

ACOUSTIC VERSUS ELASTIC WAVE PROPAGATION EFFECTS

A comparison of acoustic versus elastic responses was also made. Two cases were involved: the primaries only, and

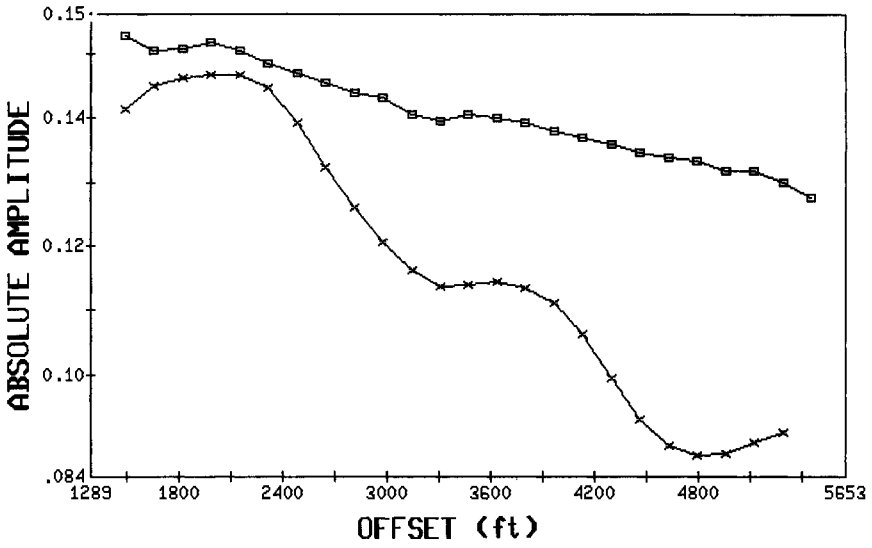

FIG. 9. Amplitudes variation with offset picked at the target horizon using the seismogram shown in Figure 8 (crosses). The amplitudes of the point-source corrected primaries were plotted for comparison (squares).

the primaries plus transmission losses and compressional interbed multiples at the target interface.

In Figure 13 the acoustic prestack synthetic seismograms for the primaries only are shown in (a) and the primaries plus transmission losses and compressional interbed multiples are shown in (b). The equivalent elastic synthetic seismograms are shown in Figures 2b and Figure 4. This comparison reveals that acoustic and elastic responses are very similar for small incidence angles, but differ for relatively large offsets. (Figure 12). Actually, in this case, acoustic theory underestimates the real offset dependent effect and produces some bias in the AVO gradient estimates that may be important.

The results of the above comparison show that corrections for the wave propagation effects should be based on an elastic approximation provided that the Q effects have been removed. Otherwise a viscoelastic approximation should be used. Corrections based on acoustic approximations will not, in general, be sufficient for relatively large offsets.

DISCUSSION AND SYNOPSIS

The wave propagation effects produce monotonic changes in the AVO behavior. These effects induce a global decrease of the amplitude variation with offset. The offset-dependent spreading losses are considerable and must not be neglected, or partially corrected, when the seismic data is to be used for AVO analysis.

Attenuation due to transmission losses, interbed multiples, and Q effects are the most important and complicated wave propagation factors affecting AVO behavior. The Q effects invariably cause decreases of amplitude with offset due to the larger propagation distances in the absence of complex structure. These effects may be reduced approximately in data processing; however, inverse modeling may be an alternative to more accurately account for the above effects (Martinez and McMechan, 1991b). Surface related multiples and P-SV-wave mode conversions interfere with the primary events, inducing large variances in the AVO

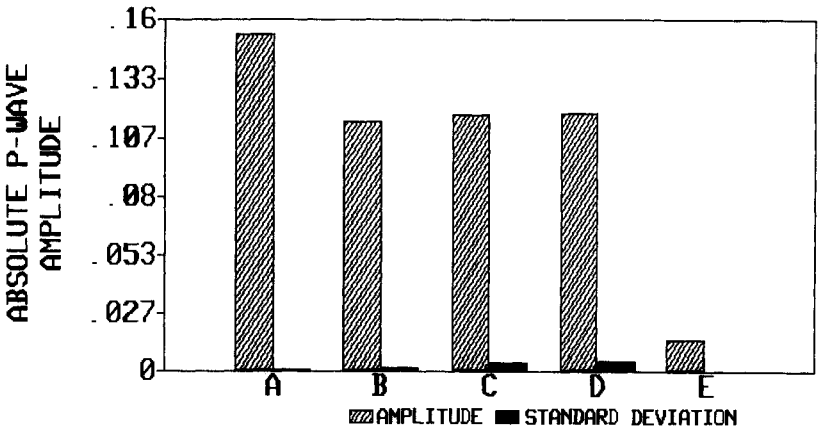

FIG. 10. AVO analysis results for the P-wave estimate and its standard deviation: (a) primaries, (b) primaries plus transmission losses and compressional interbed multiples, (c) the effects as in (b) plus compressional surface related multiples, (d) the effects as in (c) plus P-SV mode-converted waves (including multiples), and (e) the effects as in (d) plus inelastic attenuation. The spreading loss correction was applied in all cases.

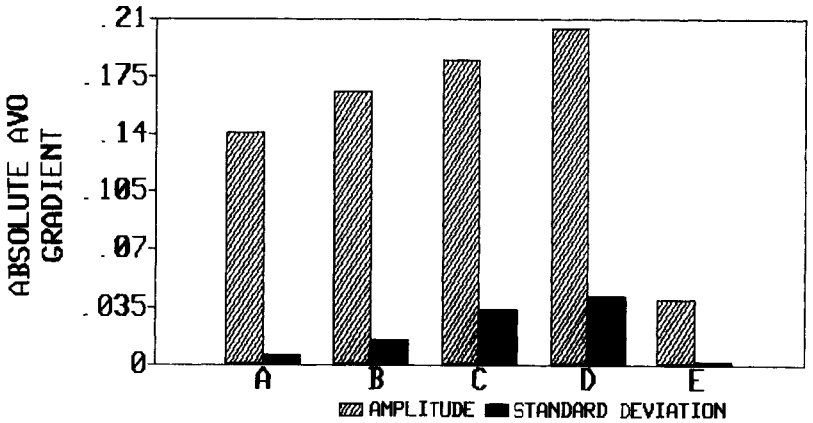

FIG. 11. AVO analysis results for the absolute AVO gradient and its standard deviation: (a) primaries, (b) primaries plus transmission losses and compressional interbed multiples, (c) the effects as in (b) plus compressional surface multiples, (d) the effects as in (c) plus P-SV mode-converted waves (including multiples), and (e) the effects as in (d) plus inelastic attenuation. The spreading loss correction was applied in all cases.

gradient estimates. This suggests that these propagation modes should be attenuated prior to AVO analysis.

The wave propagation effects are of a viscoelastic nature and are not acoustic. Acoustic approximations do not account for these effects properly, especially at relatively large offsets. Therefore, the corrections for these effects must be based on elastic approximations, provided the Q effects have been removed, otherwise they should be viscoelastic.

Finally, all the numerical experiments presented in this paper suggest that careful data processing and the right selection of processes, such as offset-dependent spreading loss corrections, prestack Q and transmission compensa-

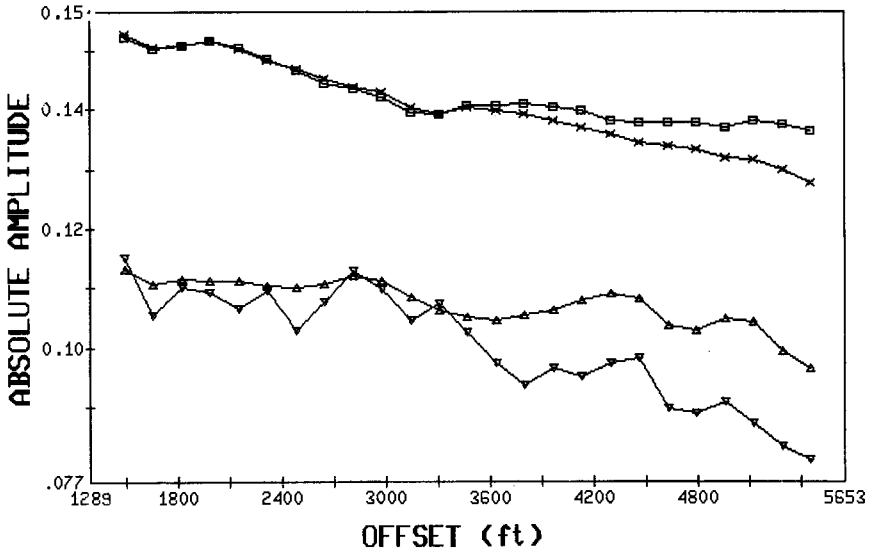

FIG. 12. Amplitudes variation with offset picked at the target horizon for the acoustic (squares and triangles) and elastic (crosses and upside down triangles) cases. The amplitudes indicated by the squares and crosses correspond to the primaries with no wave propagation effects. The amplitudes indicated by the triangles and upside down triangles correspond to the primaries plus transmission losses and interbed multiples. The spreading loss correction was applied in all cases.

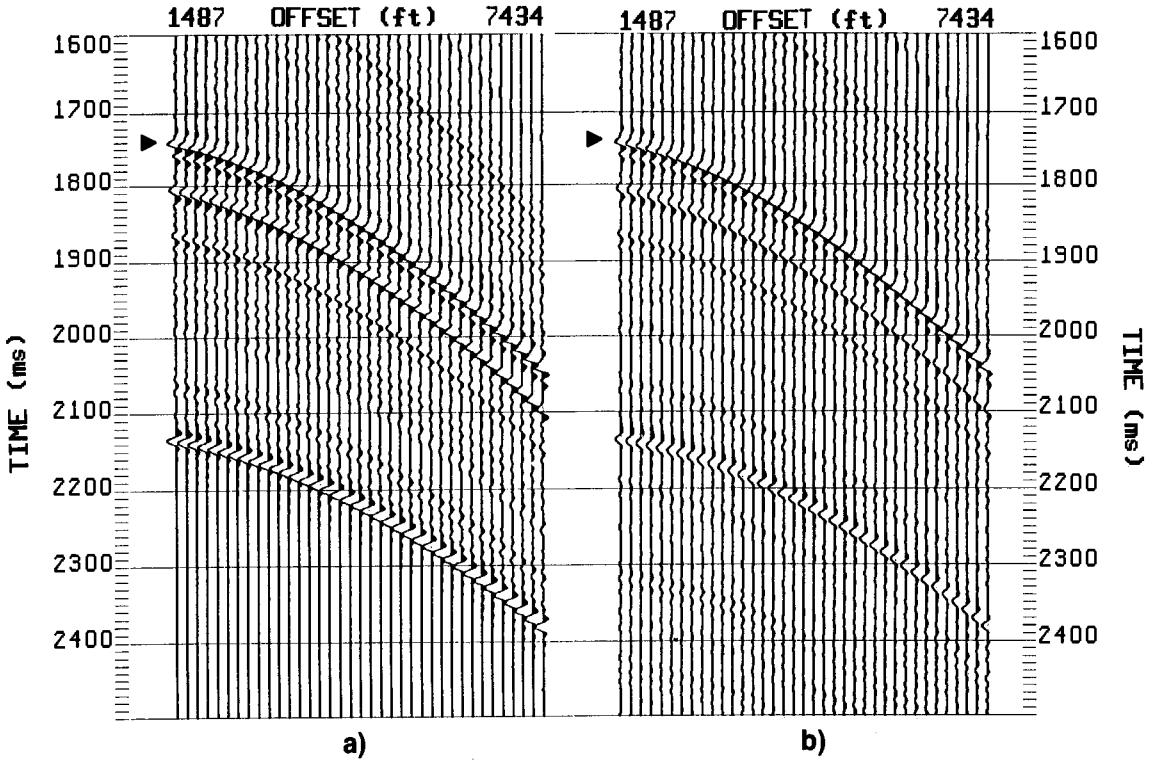

FIG. 13. Prestack acoustic synthetic seismograms: (a) primaries, (b) primaries plus transmission losses and interbed multiples. Both cases (a) and (b) were corrected for spreading losses. The arrow indicates the target horizon.

tion, and interbed multiple attenuation are necessary. Also, the attenuation of surface related multiples and noise reduction is needed to achieve successful results in AVO parameter estimation.

ACKNOWLEDGMENTS

I wish to thank Halliburton Geophysical Services (HGS) for allowing me to publish this work. I would also like to thank my colleagues at HGS, Richard Uden, Bob Seymour, Ted Shuck, Dave Monk, and Geoff Mansfield for reviewing the manuscript and for their helpful discussions. I especially thank Juergen Pruessmann of the Institut fuer Geophysik (Germany) for his valuable comments and suggestions.

REFERENCES

Berkhout, A. J., 1987, Applied seismic wave theory: Elsevier Science Publ.

Byun, B. S., and Young, C., 1989, Effects of subsurface characteristics on surface seismic measurements: A simulation study on horizontally layered media: Geophysics, **54**, 730–736.

Chacko, S., 1989, Porosity identification using amplitude variations with offset: Examples from South Sumatra: Geophysics, **54**, 942–951.

Dohr, G., 1985, Seismic shear waves: Part A: Volume **15-A**, Geophysical Press.

Fuchs, K., and Muller, G., 1971, Computation of synthetic seismograms with the reflectivity method and comparison with observations: Geophys. J. Roy. Astr. Soc., **23**, 417–433.

Gassaway, G. S., 1985, Effects of shallow reflectors on amplitude versus offset (seismic lithology) analysis: 17th Ann. Offshore Tech. Conf., 325–330.

Gassaway, G. S., Brown, R. A., and Bennett, L. E., 1986. Pitfalls in seismic amplitude versus offset analysis: Case histories: 18th Ann. Offshore Tech. Conf., 481–487.

Han, D. H., Nur, A., and Morgan, D., 1986, Effects of clay content on wave velocities in sandstones: Geophysics, **51**, 2093–2107.

Kennett, B. N. L., 1979, Theoretical reflection seismograms for elastic media: Geophys. Prosp., **27**, 301–321.

Krail, P. M., and Shin, Y., 1990, Deconvolution of a directional marine source: Geophysics, **55**, 1542–1548.

MacLeod, M. K., and Martin, H. L., 1988, Amplitude changes due to bed curvature: 58th Ann. Internat. Mtg., Soc. Expl. Geophys., Expanded Abstracts, 1209–1212.

Martinez, R. D., and McMechan, G. A., 1987, Analysis of absorption and dispersion effects using τ-p synthetic seismograms: Geophysics, **52**, 1033–1047.

——— 1991a, τ-p seismic data for viscoelastic media—Part 1: Modeling: Geophys. Prosp., **39**, 141–156.

——— 1991b, τ-p seismic data for viscoelastic media—Part 2: Linearized inversion: Geophys. Prosp., **39**, 157–182.

Ostrander, W., 1984, Plane-wave reflection coefficients for gas sands at nonnormal angles of incidence: Geophysics, **49**, 1637–1648.

Pruessmann, J., and Behle, A., 1990, Offset-dependence of stratigraphic attenuation in a finely-layered subsurface: Presented at the 52nd Ann. Internat. Mtg., European Assoc. Expl. Geophys.

Resnick, J. R., Ng P., and Larner, K., 1987, Amplitude versus offset analysis in the presence of dip: 57th Ann. Internat. Mtg., Soc. Expl. Geophys., Expanded Abstracts, 617–620.

Rutherford S. R., and Williams, R. H., 1989, Amplitude versus offset variations in gas sands: Geophysics, **54**, 680–688.

Sheriff, R. E., 1975, Factors affecting seismic amplitudes: Geophys. Prosp., **23**, 125–138.

Silva, R., and Ahmed, H., 1989, Application of the AVO technique in production geophysics: 59th Ann. Internat. Mtg., Soc. Expl. Geophys., Expanded Abstracts, 836–838.

Spratt, S., 1987, Effect of normal moveout errors on amplitude versus offset-derived shear reflectivity: 57th Ann. Internat. Mtg., Soc. Expl. Geophys., Expanded Abstracts, 634–637.

Swan, H. W., 1991, Amplitude versus offset measurement errors in a finely layered medium: Geophysics, **56**, 41–49.

Shuey, R., 1985, A simplification of Zoeppritz equations: Geophysics, **50**, 609–614.

Ursin, B., 1990, Offset-dependent geometrical spreading in a layered medium: Geophysics, **55**, 492–496.

Walden, A. T., 1990, Making AVO sections more robust: Presented at the 52nd Ann. Internat. Mtg., European Assoc. Expl. Geophys.

Yu, G., 1985, Offset-amplitude variation and controlled amplitude processing: Geophysics, **50**, 2697–2708.